



HAL
open science

Influence of nitrogen impurities on the formation of active species in Ar-O plasmas

V. Guerra, K. Kutasi, P.A. Sá, M. Lino da Silva

► **To cite this version:**

V. Guerra, K. Kutasi, P.A. Sá, M. Lino da Silva. Influence of nitrogen impurities on the formation of active species in Ar-O plasmas. *European Physical Journal: Applied Physics*, 2011, 56 (2), pp.24004. 10.1051/epjap/2011110194 . hal-00746213

HAL Id: hal-00746213

<https://hal.science/hal-00746213>

Submitted on 28 Oct 2012

HAL is a multi-disciplinary open access archive for the deposit and dissemination of scientific research documents, whether they are published or not. The documents may come from teaching and research institutions in France or abroad, or from public or private research centers.

L'archive ouverte pluridisciplinaire **HAL**, est destinée au dépôt et à la diffusion de documents scientifiques de niveau recherche, publiés ou non, émanant des établissements d'enseignement et de recherche français ou étrangers, des laboratoires publics ou privés.

Influence of nitrogen impurities on the formation of active species in Ar-O₂ plasmas

Vasco Guerra^{1,2}, Kinga Kutasi³, Paulo A. Sá^{1,4}, and M. Lino da Silva¹

¹ Instituto de Plasmas e Fusão Nuclear, Instituto Superior Técnico, 1049-001 Lisboa, Portugal

² Departamento de Física, IST, Universidade Técnica de Lisboa, Portugal

³ Research Institute for Solid State Physics and Optics, Hungarian Academy of Sciences, POB 49, H-1525 Budapest, Hungary

⁴ Departamento de Engenharia Física, Faculdade de Engenharia da Universidade do Porto, 4200-465 Porto, Portugal

Received: date / Revised version: date

Abstract. A self-consistent kinetic model was developed in order to study the production of active species in Ar-O₂ surface-wave microwave plasmas with a relatively small N₂ addition. It is shown that the Ar-O₂-N₂ mixture produces efficiently the same active species as an Ar-O₂ discharge, including oxygen atoms, metastable O₂(*a* ¹Δ_g) molecules and the VUV emitting Ar(4s) states. Furthermore, active N-containing species are additionally produced, in particular N atoms and NO ground-state and excited molecules, which makes the ternary mixture very interesting for numerous plasma applications.

1 Introduction

Low-pressure Ar-O₂ surface-wave microwave discharges and their afterglows are very efficient sources of active species, such as O(³P) atoms, O₂(*a* ¹Δ_g) and O₂(*b* ¹Σ_g⁺) metastables, ozone, metastable Ar(³P₂, ³P₀) and resonant Ar(³P₁, ¹P₁) argon atoms, as well as a variety of ions. They are thus interesting for several applications, for instance plasma sterilization [1–5], synthesis of nanowires [6,7], wool treatment [8], different surface treatment processes [9–15], damaging of cancer cells [16,17] or the iodine-

oxygen laser excitation [18–21]. We have recently conducted a thorough theoretical investigation on the formation of active species in these discharges [22,23], discussing in detail their main creation and destruction mechanisms and the conditions where they can be efficiently produced. However, nitrogen impurities are often present in Ar, O₂ or Ar-O₂ discharges, as confirmed by the frequent experimental detection of the emission of N-containing species. The purpose of this work is to address this issue, by extending our previous models to the case of Ar-O₂-N₂ mixtures and by studying the influence of a small addition of

nitrogen into an Ar-O₂ discharge. Our analysis is twofold. On the one hand, we want to verify up to what point a small addition of nitrogen may affect the existing Ar-O₂ active species which are important for the various applications. On the other hand, we want to determine if the presence of nitrogen may lead to the significant production of other active species, namely N(⁴S) atoms, N₂(A) metastables and NO excited molecules, which may have a role in processing.

The system under analysis consists of a surface-wave discharge created by a microwave field at $f = 2.45$ GHz in a 5 mm inner diameter cylindrical quartz tube at $p = 4$ mbar. The working gas mixture is 10%O₂–90%Ar, into which nitrogen is added. Therefore, the initial Ar to O₂ ratio is always kept at 9:1, and the notation %N₂ refers to the initial nitrogen concentration in the mixture. These operating conditions correspond to the ones used in [24, 11] in surface contamination cleaning and sterilization experiments. The delivered microwave power in the experiments from [11] was 100 W.

The remaining of the paper is organized as follows. Section 2 shortly describes the kinetic model developed in this study. The results and their discussion are presented in section 3. Finally, the results are briefly summarized in section 4.

2 Theoretical model

The structure of the model was described in detail in previous publications. Basically, the homogeneous electron Boltzmann equation is solved in the two-term expansion

in spherical harmonics, coupled with a set of rate balance equations describing the creation and loss of the most important neutral and ionic species, including the molecular excited states O₂($a^1\Delta_g, b^1\Sigma_g^+$), N₂($A^3\Sigma_u^+, B^3\Pi_g, C^3\Pi_u, a'^1\Sigma_u^-, a^1\Pi_g, w^1\Delta_u$) and NO(A, B), ground-state Ar(¹S₀), O(³P) and N(⁴S) atoms, excited Ar(³P₂, ³P₁, ³P₀, ¹P₁), O(¹D) and N(²D, ²P) atoms, NO(X) and O₃ molecules, the manifold of vibrational N₂($X^1\Sigma_g^+, v$) levels, and Ar⁺, Ar₂⁺, O⁺, O₂⁺, N₂⁺, N₄⁺, NO⁺ and O⁻ ions. The full set of reactions considered in the Ar-O₂ system is detailed in [22, 23]. Information related to the N₂-Ar reactions can be found in [25–27], to the N₂-O₂ kinetics in [28–30], and to the vibration kinetics and the calculation of the vibration levels in [31, 32]. The system of equations is solved in stationary discharge conditions, considering an electron density corresponding to the critical density for surface-wave propagation, $n_e = 3.74 \times 10^{11}$ cm⁻³ [22], describing approximately the conditions at the end of the plasma column. All the calculations in the discharge were performed assuming a gas temperature $T_g = 500$ K [33, 23], but the sensitivity of the model to the value used for the gas temperature is briefly evaluated in the end of the next section. The concentrations obtained from the stationary model can then be used as initial values for the time relaxation in the afterglow, where the same system of rate balance equations is solved for the heavy-particles together with the continuity equation for the electron density, neglecting all electron impact excitation, dissociation and ionization processes. Notice, however, that electron-ion recombination is included in the system of rate balance

equations in the post-discharge [23]. The gas temperature in the afterglow was assumed to be $T_g = 300$ K. The time-dependent calculated profiles can be converted into spacial-dependent profiles by knowing the gas flow.

A relevant phenomenon can be the modification of the oxygen atomic wall recombination probability, γ_O , with the presence of small amounts of nitrogen. Indeed, a pronounced decrease of this recombination probability was found and discussed in [34–36]. A review on literature data and further discussion of this topic can be found in [37].

A correct treatment of this question involves the coupling of the present model to a system of equations describing the surface kinetics, such as the ones presented in [36, 38]. However, the uncertainties surrounding the data of the elementary surface processes recommend the use of surface models only if accompanied by a comparison with a consistent set of measurements for the particular conditions under study. As such measurements are currently unavailable, the present results were obtained considering a constant value for γ_O , equal to 8×10^{-3} [39]. A more detailed analysis of the modifications in γ_O as a result of the presence of impurities, as well as the impact in the overall composition of the plasma, will be performed in future.

3 Results and discussion

Our models have been validated in previous publications by a systematic comparison with very complete sets of measurements in various operating conditions, both in pure gases and in Ar-N₂ and N₂-O₂ mixtures. The com-

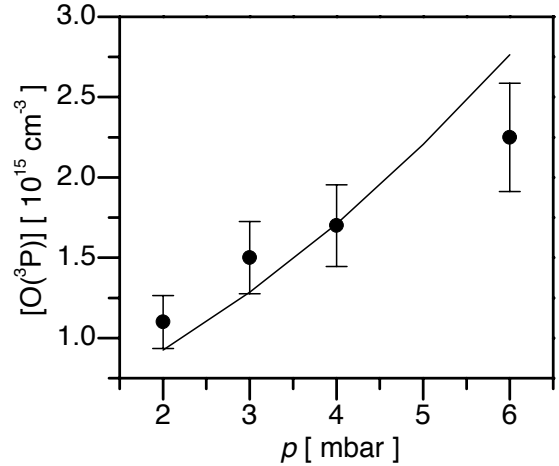
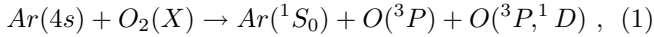


Fig. 1. $O(^3P)$ concentration as a function of pressure: the full curves are the model results, the experimental points with error bars are the measurements reported in [11] for the afterglow. The delivered microwave power was 100 W.

plete list of references would be too long to include here, so references [40–43] should merely be seen as supplementary examples. However, despite the importance of Ar-O₂-N₂ surface-wave discharges and their afterglows for many applications, the experimental characterization of the active species for the conditions of this study is relatively poor.

A comparison of our calculations with most of the few available data for the Ar-O₂ mixture is presented in [22, 23]. An additional comparison between the model predictions and the experimental measurements is now shown in figure 1. The experimental points with error bars are taken from [11] and correspond to a position of 45 cm from the plasma gap. We estimate this corresponds to an afterglow time of about 2 ms. Nevertheless, it must be noted that there are large uncertainties on the time-space conversion, mostly related to the determination of the plasma column

end and the gas temperature, both values being modified with pressure and affecting the afterglow time corresponding to a certain position. Still, the agreement between the calculations and the measurements is remarkably good. As pointed out in [22], in discharges containing 90% argon, O(³P) atoms are formed both by electron impact dissociation of O₂(X, a, b) molecules and dissociation in collisions with the Ar(4s) states,



the two channels giving comparable contributions to the formation of atomic oxygen, whereas they are essentially destroyed by recombination at the wall. Anyhow, the behavior of the dissociation with pressure is in general rather complex and, together with a more accurate afterglow space-time conversion, will be investigated in detail in a future publication.

The influence of nitrogen addition into a 90%Ar-10%O₂ discharge can be evaluated in figures 2-7. Figure 2 shows the concentration of the Ar(4s) states as a function of the nitrogen concentration in the mixture. As it can be seen, the absolute concentration of excited argon atoms remains practically constant. Notice that the addition of nitrogen does not modify the kinetics of the Ar(4s) states, whereas the sustaining reduced field slightly increases with the nitrogen concentration in the mixture as a result of the higher electron-impact cross sections in nitrogen. As a matter of fact, these higher cross sections lead to a more effective depopulation of the high-energy tail of the Electron Energy Distribution Function (EEDF), so that the

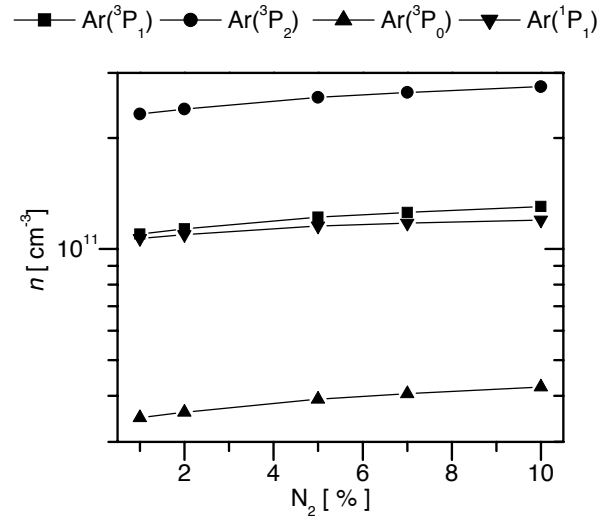
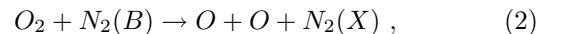


Fig. 2. Concentration of the Ar(4s) states at the end of the plasma column as a function of the nitrogen content in the mixture, for $p = 4$ mbar and an initial Ar to O₂ ratio of 9:1.

reduced maintenance electric field has to increase in order to keep the same ionization degree [28,22].

The effect of the nitrogen content on the oxygen species can be verified in figure 3. As in the previous case, the introduction of up to 10% of nitrogen in the mixture has a negligible effect in the concentration of the active species. Most of the new reactions taking place contribute less than one percent to the formation or destruction of the oxygen species. Still, at 10% N₂ in the mixture, dissociation of O₂ by N₂(B) molecules,



gives ~ 3% to the formation of atomic oxygen.

Figure 4 depicts the concentration of the nitrogen containing species, allowing to evaluate up to which point they can be used in plasma processing. Nitrogen atoms are particularly important, their population increasing more

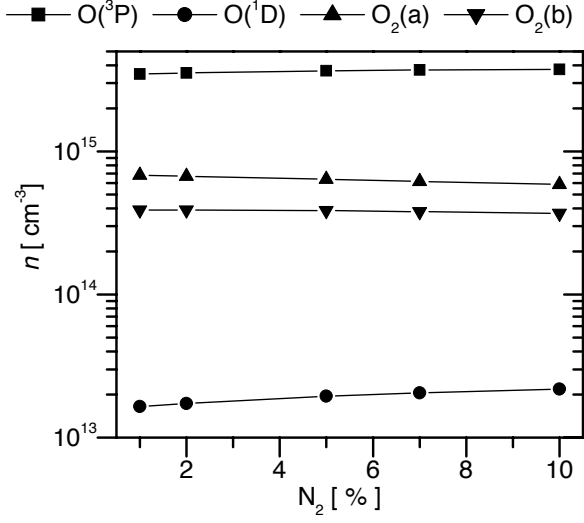


Fig. 3. Concentration of the oxygen species at the end of the plasma column as a function of the nitrogen content in the mixture, for $p = 4$ mbar and an initial Ar to O₂ ratio of 9:1.

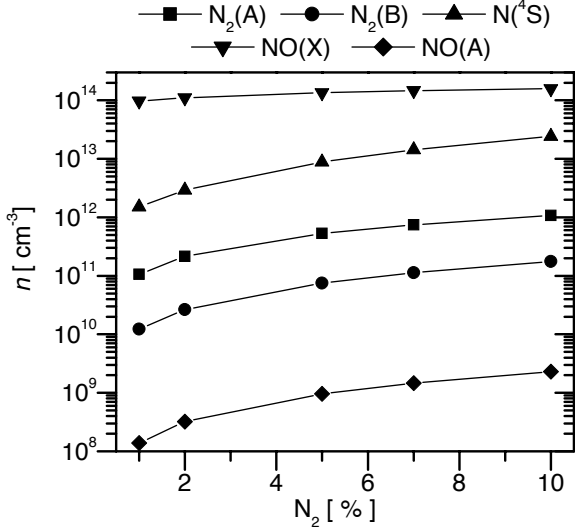
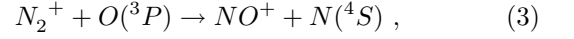
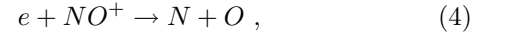


Fig. 4. Concentration of N-containing species at the end of the plasma column as a function of the nitrogen content in the mixture, for $p = 4$ mbar and an initial Ar to O₂ ratio of 9:1.

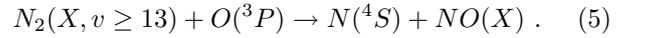
than one order of magnitude when the nitrogen fraction raises from 1 to 10%. The contribution of different processes to the formation of atomic nitrogen is represented in figure 5. At low N₂ percentages, nitrogen atoms are mainly formed by electron impact dissociation, charge transfer from N₂⁺ to NO⁺,



and total quenching (volume quenching by heavy-particles and electrons and surface quenching) of the metastable atomic state N(²D). At this low concentrations of N₂, electron-ion recombination



with a rate of the order of 2×10^{-8} cm³/s for an electron temperature ~ 1 eV, gives also a non-negligible contribution close to 10%; however, its importance quickly decreases with N₂ addition. At 10% N₂ in the mixture, the dominant N(⁴S) creation mechanism becomes the reaction of NO production



The strong increase of the importance of this process is the most striking feature revealed by figure 5. Other important contributions come from electron impact dissociation and the aforementioned charge transfer process.

Another relevant species is NO. Its formation channels are also modified when the N₂ content increases, as it can be seen in figure 6. Thus, for low N₂ concentrations it is essentially created by NO⁺ neutralization at the wall and

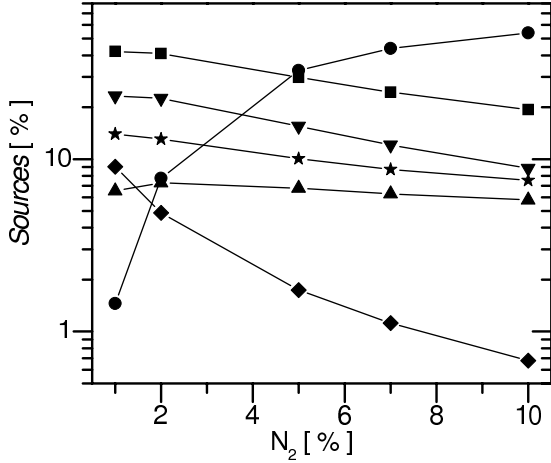
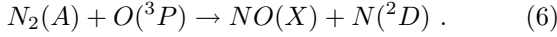


Fig. 5. Contribution of different mechanisms to the formation of N atoms, for $p = 4$ mbar and an initial Ar to O₂ ratio of 9:1: (■) electron impact dissociation; (●) $N_2(X, v \geq 13) + O(^3P) \rightarrow N(^4S) + NO(X)$; (▲) $N_2(a') + NO \rightarrow N + O$; (▼) $N_2^+ + O(^3P) \rightarrow NO^+ + N(^4S)$; (◆) $e + NO^+ \rightarrow N + O$; (★) wall and volume quenching of $N(^2D)$ atoms.

by the formation reaction involving $N_2(A)$ molecules



In contrast, at higher N_2 fractions it is dominantly formed by the reaction involving vibrationally excited nitrogen molecules (5), the other two mechanisms just referred to giving as well non-negligible contributions. Further discussion on the competition between processes (5) and (6) can be found in [44, 45]. The raise in importance of reaction (5) with the nitrogen content previously noted in figure (5) is clearly visible. It is a consequence of the strong enhancement of the fraction of vibrationally excited ground-state $N_2(X, v)$ nitrogen molecules in levels $v \geq 13$, which increases almost two orders of magnitude, from 4.7×10^{-4} to 3.5×10^{-2} , when the nitrogen percentage in the mixture goes from 1 to 10%.

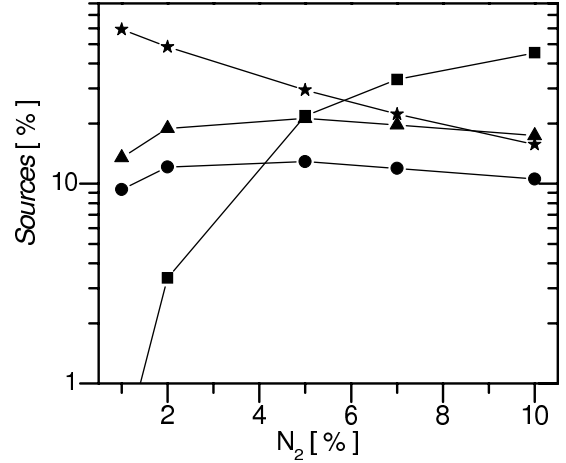
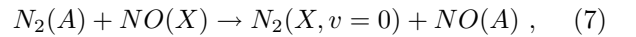


Fig. 6. Contribution of different mechanisms to the formation of NO molecules, for $p = 4$ mbar and an initial Ar to O₂ ratio of 9:1: (■) $N_2(X, v \geq 13) + O(^3P) \rightarrow N(^4S) + NO(X)$; (●) $N(^2D) + O_2 \rightarrow NO + N(^4S)$; (▲) $N_2(A) + O(^3P) \rightarrow NO(X) + N(^2D)$; (★) wall neutralization of NO^+ ions.

It is also worth noting that UV emitting $NO(A)$ molecules reach densities of the order of 10^9 cm^{-3} . Such population already provides a reasonable emission intensity, of special interest in biomedical applications and surface treatments. The kinetics of $NO(A)$ is relatively simple, as this state is produced by the collisional energy transfer



being destroyed by radiative decay and, in a smaller extent, by quenching with O₂ molecules.

Figure 7 exhibits the ionic composition of the mixture. As it could be concluded from the discussion of the previous results, NO^+ quickly becomes the dominant ion, therefore playing a relevant role in the kinetics of several species. This is fundamentally a consequence of the very efficient charge transfer from O_2^+ and N_2^+ ions into NO^+ [46].

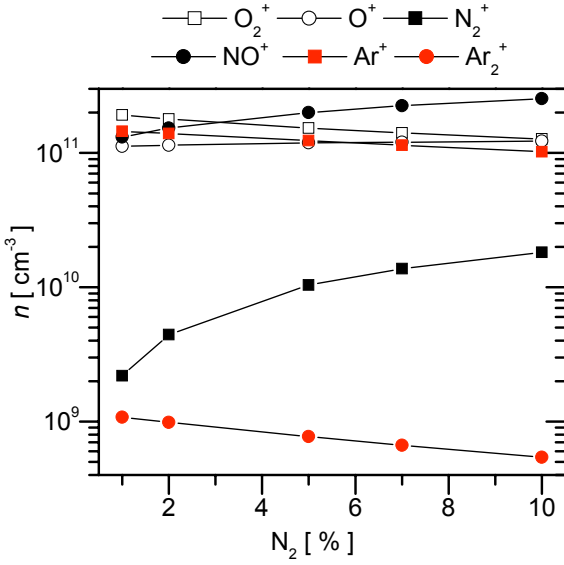


Fig. 7. Ionic populations at the end of the plasma column as a function of the nitrogen content in the mixture, for $p = 4$ mbar and an initial Ar to O₂ ratio of 9:1.

As the calculations have been made at constant gas temperature, $T_g = 500$ K, it is important to estimate the influence of the gas temperature on the calculations. To this purpose, we have made the calculations using $T_g = 700$ K, for the cases of 1% and 5% N₂ in the mixture. The profiles of the different species are not modified, and the changes in the concentrations are rather small. For instance, for 1% N₂ in the mixture the relative concentration of atomic nitrogen (oxygen) is changed from 2.6×10^{-5} (6.0×10^{-2}) to 3.1×10^{-5} (5.5×10^{-2}) when the gas temperature increases from 500 K to 700 K, respectively, while it goes from 1.4×10^{-4} (6.3×10^{-2}) to 1.7×10^{-4} (5.9×10^{-2}) in the 5% N₂ mixture.

4 Conclusion

In this work we have extended our previous models [22, 23] to study the influence of nitrogen addition in Ar-O₂ discharges. The conditions of this investigation were the same as in the experiments from [24, 11], namely a microwave surface-wave discharge at $p = 4$ mbar, with field frequency $f = 2.45$ GHz and nitrogen introduction into a 90%Ar-10%O₂ mixture. It was shown that the concentration of argon and oxygen active species is not significantly modified by the introduction of up to 10% N₂ in the mixture. Moreover, other species with potential interest in technological applications, such as NO(*X*, *A*, *B*) molecules, N(⁴S) atoms and NO⁺ ions, are additionally produced. Therefore, the ternary mixture Ar-O₂-N₂ can indeed be advantageously used in several plasma processes, as suggested in [47–49] and pointed out in [22, 23].

Future work shall concentrate in finding the optimal conditions for the production of specific species required for a particular application and in investigating their time-evolution and survival time in the afterglow. The role of surface processes in the formation of molecules is also a pressing topic to be addressed [36, 50].

Acknowledgement

The work has been supported by the Portuguese Fundação para a Ciência e Tecnologia (FCT) funds to Instituto de Plasmas e Fusão Nuclear – Laboratório Associado and by the Janos Bolyai Research Scholarship of the Hungarian Academy of Sciences.

References

1. Moreau S, Moisan M, Tabrizian M, Barbeau J, Pelletier J, Ricard A, and Yahia L 2000 *J. Appl. Phys.* **88** 1166–1174
2. Nagatsu M, Terashita F, Nonaka H, Xu L, Nagata T and Koide Y 2005 *Appl. Phys. Lett.* **86** 211502
3. Rossi F, Kylián O and Hasiwa M 2006 *Plasma Process. Polym.* **3** 431–442
4. Raballand V, Benedikt J, Wunderlich J and von Keudell A 2008 *J. Phys. D: Appl. Phys.* **41** 115207
5. Vratnica Z, Vujošević D, Cvelbar U and Mozetič M 2008 *IEEE Trans. Plasma Sci.* **36** 1300–1301
6. Mozetič M, Cvelbar U, Sunkara M and Vaddiraju S 2005 *Adv. Mater.* **17** 2138–2142
7. Cvelbar U, Ostrikov K and Mozetič M 2008 *Nanotechnology* **19** 405605
8. Canal C, Gaboriau F, Ricard A, Mozetic M, Cvelbar U and Drenik A 2007 *Plasma Chem. Plasma Process.* **27** 404–413
9. Belmonte T, Czerwiec T, Gavillet J and Michel H 1997 *Surface Coat. Technol.* **97** 642–648
10. Puač N, Petrović Z, Radetić M and Djordjević A 2005 *Mater. Sci. Forum* **494** 291–296
11. Mafra M, Belmonte T, Poncin-Epaillard F, Maliska A and Cvelbar U 2009 *Plasma Process. Polym.* **6** S198–S203
12. Klanjšek-Gunde M, Kunaver M, Hrovat A and Cvelbar U 2005 *Prog. Org. Coat.* **54** 113–119
13. Kitajima T, Nakano T and Makabe T 2006 *Appl. Phys. Lett.* **88** 091501
14. Mozetic M, Zalar A, Cvelbar U and Babic D 2004 *Surf. Interface Anal.* **36** 986–988
15. Vesel A, Drenik A, Mozetic M, Zalar A, Balat-Pichelin M and Bele M 2007 *Vacuum* **82** 228–231
16. Parker J G 1984 *John Hopkins APL Technical Digest* **5** 48–50
17. Niedre M J, Yu C S, Patterson M S and Wilson B C 2005 *British J. Cancer* **92** 298–304
18. Ionin A A, Kochetov I V, Napartovich A P and Yuryshev N N 2007 *J. Phys. D: Appl. Phys.* **40** R25–R61
19. Woodard B S, Zimmerman J W, Benavides G F, Carroll D L, Verdeyen J T, Palla A D, Field T H, Solomon W C, Lee S, Rawlins W T and Davis S J 2010 *J. Phys. D: Appl. Phys.* **43** 025208
20. Hicks A, Bruzzese J R and Adamovich I V 2010 *J. Phys. D: Appl. Phys.* **43** 025206
21. Guerra V, Kutasi K and Sá P A 2010 *Appl. Phys. Lett.* **96** 071503
22. Kutasi K, Guerra V and Sá P 2010 *J. Phys. D: Appl. Phys.* **43** 175201
23. Kutasi K, Guerra V and Sá P A 2011 *Plasma Sources Sci. Technol.* **20** 035006
24. Ricard A and Monna V 2002 *Plasma Sources Sci. Technol.* **11** A150–A153
25. Sá P A and Loureiro J 1997 *J. Phys. D: Appl. Phys.* **30** 2320–2330
26. Henriques J, Tatarova E, VGuerra and Ferreira C M 2002 *J. Appl. Phys.* **91** 5622–5631
27. Henriques J, Tatarova E, Dias F M and Ferreira C M 2002 *J. Appl. Phys.* **91** 5632–5639
28. Guerra V and Loureiro J 1997 *Plasma Sources Sci. Technol.* **6** 373–385
29. Pintassilgo C D, Loureiro J and Guerra V 2005 *J. Phys. D: Appl. Phys.* **38** 417
30. Kutasi K, Saoudi B, Pintassilgo C D, Loureiro J and Moisan M 2008 *Plasma Process. Polym.* **5** 840–852

31. Loureiro J and Ferreira C M 1986 *J. Phys. D: Appl. Phys.* **19** 17–35
32. Lino da Silva M, Guerra V, Loureiro J and Sá P A 2008 *Chem. Phys.* **348** 187
33. Tatarova E, Dias F M, Ferreira C M and Ricard A 1999 *J. Appl. Phys.* **85** 49–62
34. Dilecce G and Benedictis S D 1999 *Plasma Sources Sci. Technol.* **8** 266–278
35. Gordiets B F, Ferreira C M, Nahorny J, Pagnon D, Touzeau M and Vialle M 1996 *J. Phys. D: Appl. Phys.* **29** 1021–1031
36. Gordiets B F and Ferreira C M 1998 *AIAA Journal* **36** 1643–1651
37. Kutasi K and Loureiro J 2007 *J. Phys. D: Appl. Phys.* **40** 5612–5623
38. Guerra V 2007 *IEEE Trans. Plasma Sci.* **35** 1397–1412
39. Macko P, Veis P and Cernogora G 2004 *Plasma Sources Sci. Technol.* **13** 251–262
40. Henriques J, Tatarova E, Dias F M and Ferreira C M 2001 *J. Appl. Phys.* **90** 4921–4928
41. Pinheiro M J, Gousset G, Granier A and Ferreira C M 1998 *Plasma Sources Sci. Technol.* **7** 524–536
42. Guerra V, Tatarova E, Dias F M and Ferreira C M 2002 *J. Appl. Phys.* **91** 2648–2661
43. Guerra V, Sá P A and Loureiro J 2004 *Eur. Phys. J. Appl. Phys.* **28** 125–152
44. Pintassilgo C D, Guaitella O and Rousseau A 2009 *Plasma Sources Sci. Technol.* **18** 025005
45. Welzel S, Guaitella O, Lazzaroni C, Pintassilgo C D, Rousseau A and Röpcke J 2011 *Plasma Sources Sci. Technol.* **20** 015020
46. Guerra V and Loureiro J 1999 *Plasma Sources Sci. Technol.* **6** 373–385
47. Stapelmann K, Kylián O, Denis B and Rossi F 2008 *J. Phys. D: Appl. Phys.* **41** 192005
48. Kylián O and Rossi F 2009 *J. Phys. D: Appl. Phys.* **42** 085207
49. Bernardelli E A, Ricard A and Belmonte T 2011 *Plasma Sources Sci. Technol.* **20** 025012
50. Guaitella O, Hübner M, Welzel S, Marinov D, Röpcke J and Rousseau A 2010 *Plasma Sources Sci. Technol.* **19** 45026